Charge Inversion Phenomenon

SEOK, SANGJUN

IHS
SOGANG UNIVERSITY

Electric double layer model

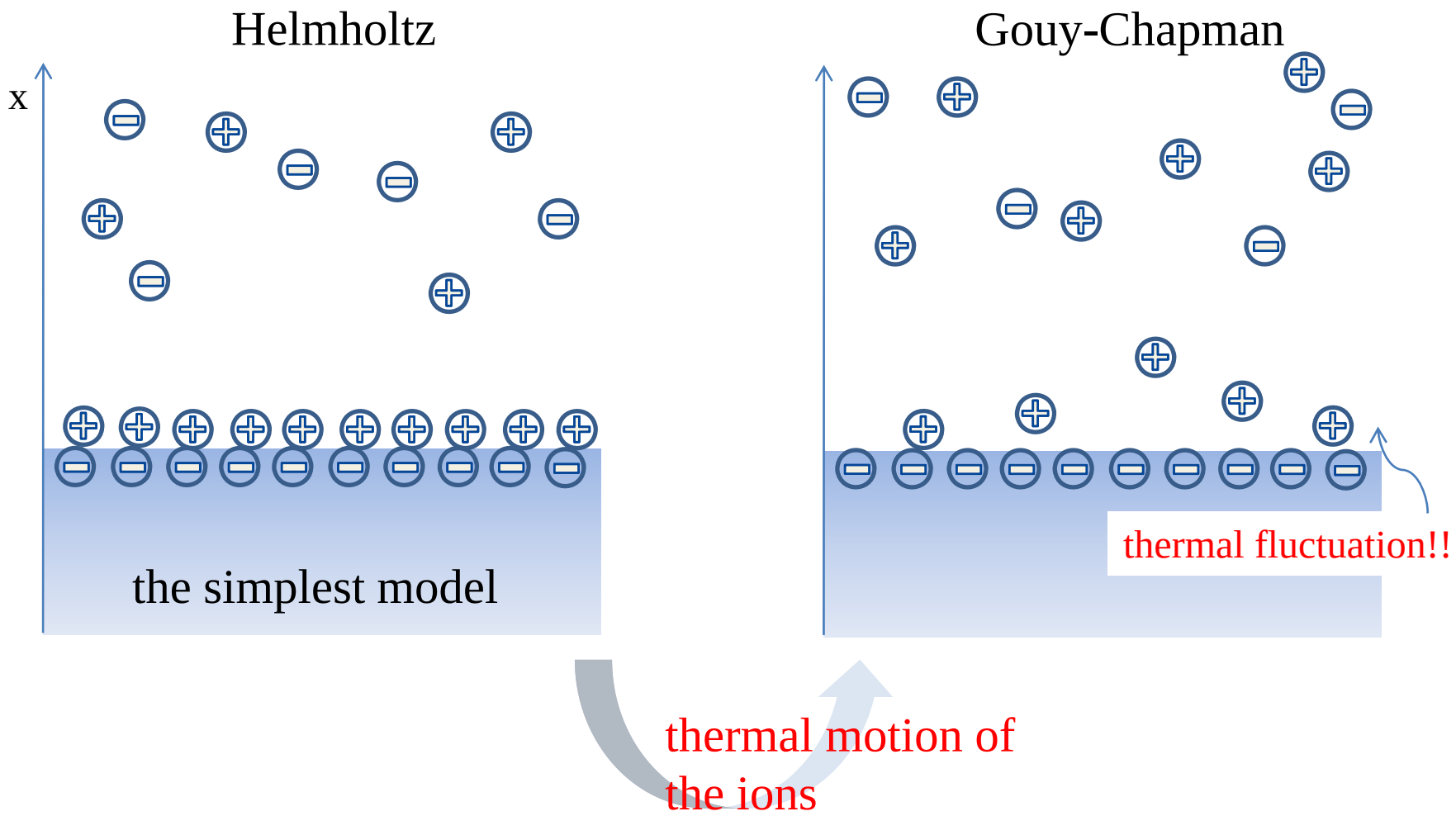

SOGANG UNIVERSITY

Poisson-Boltzmann theory – diffusive double layer

What is the potential distribution in the solution?? (on the 1:1 salt)

$$\nabla^2\varphi = \frac{\partial^2\varphi}{\partial x^2}+\frac{\partial^2\varphi}{\partial y^2}+\frac{\partial^2\varphi}{\partial z^2} = -\frac{\rho}{\varepsilon\varepsilon_0}$$

$$\rho = e(c^+ - c^-) = c_0 e\cdot\left(e^{-\frac{e\varphi(x,y,z)}{k_BT}} - e^{\frac{e\varphi(x,y,z)}{k_BT}}\right)$$

$$c^- = c_0\cdot e^{e\varphi/k_BT} \text{ and } c^+ = c_0\cdot e^{e\varphi/k_BT}$$

$$\therefore \nabla^2\varphi = \frac{c_0 e}{\varepsilon\varepsilon_0}\cdot\left(e^{\frac{e\varphi}{k_BT}} - e^{-\frac{e\varphi}{k_BT}}\right)$$

SOGANG UNIVERSITY

Poisson-Boltzmann theory – diffusive double layer

$$\nabla^2\varphi = \frac{c_0 e}{\varepsilon\varepsilon_0}\cdot\left(e^{\frac{e\varphi}{k_B T}} - e^{-\frac{e\varphi}{k_B T}}\right)$$

At room temperature

$$\varphi \le 25mV$$

linearized Poisson Boltzmann equation (Debye Hückel approximation)

$$\nabla^2\varphi = \frac{c_0 e}{\varepsilon\varepsilon_0}\cdot\left(e^{\frac{e\varphi}{k_B T}} - e^{-\frac{e\varphi}{k_B T}}\right) \approx \frac{2c_0 e^2}{\varepsilon\varepsilon_0 k_B T}\cdot\varphi$$

Debye length

$$\varphi = \varphi_0 \cdot e^{-\kappa x} \quad \leftarrow \quad \kappa = \sqrt{\frac{2c_0 e^2}{\varepsilon\varepsilon_0 k_B T}} \quad \rightarrow \quad \boxed{\lambda_D = \kappa^{-1}}$$

SOGANG UNIVERSITY

Poisson-Boltzmann theory – diffusive double layer

e.g. potential versus distance for a surface potential (surface potential 50 mV)

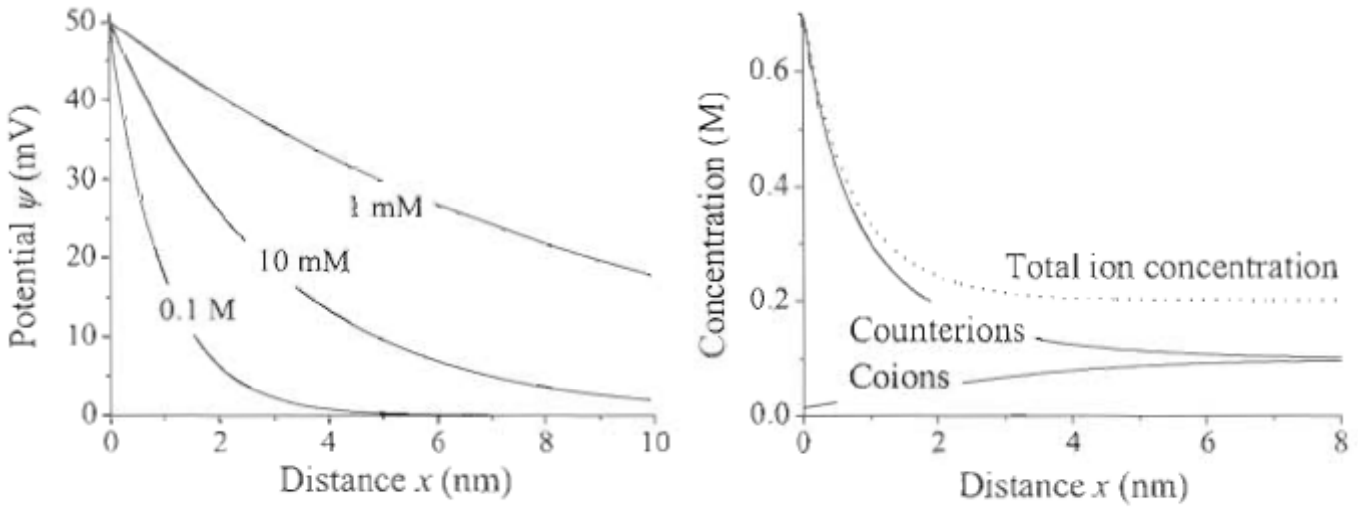

Figure 4.2: Left: Potential-versus-distance for a surface potential of $\psi_0 = 50$ mV and different concentrations of a monovalent salt in water. Right: Local co- and counterion concentrations are shown for a monovalent salt at a bulk concentration of 0.1 M and a surface potential of 50 mV. In addition, the total concentration of ions, that is the sum of the co- and counterion concentrations, is plotted.

H. Butt, K. Graf, M Kapple, physics and chemistry of interface, WILEY-VCH (2006)

SOGANG UNIVERSITY

Poisson-Boltzmann theory – diffusive double layer

e.g. potential versus distance for a surface potential (different surface potential)

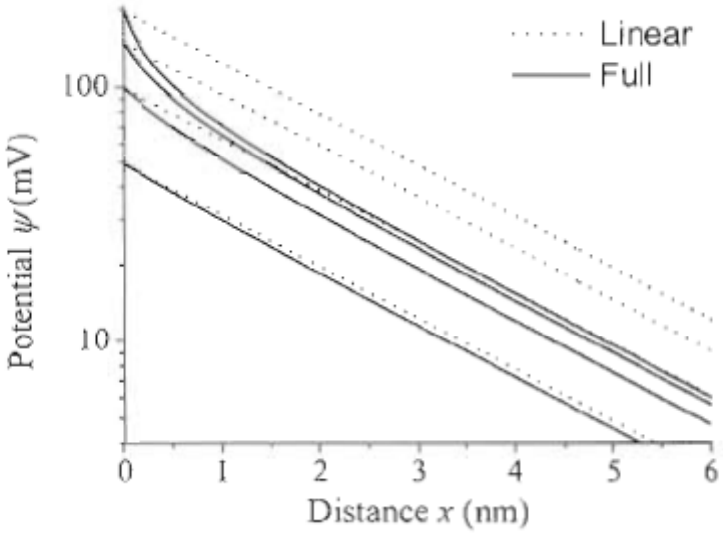

Figure 4.3: Potential-versus-distance for different surface potentials (50, 100, 150, and 200 mV) with 20 mM monovalent salt. The full solution Eq. (4.21) and the solution of the linearized Poisson–Boltzmann Eq. (4.9) are shown.

H. Butt, K. Graf, M Kapple, physics and chemistry of interface, WILEY-VCH (2006)

SOGANG UNIVERSITY

Stern layer

somewhat artificial!!

Helmholtz plane (stern layer)

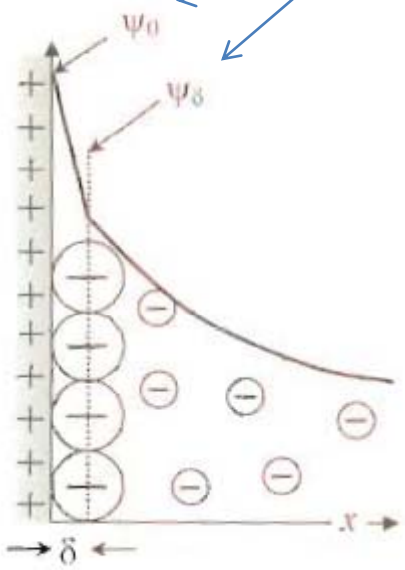

Figure 4.5: Simple version of the Stern layer.

H. Butt, K. Graf, M Kapple, physics and chemistry of interface, WILEY-VCH (2006)

Stern layer

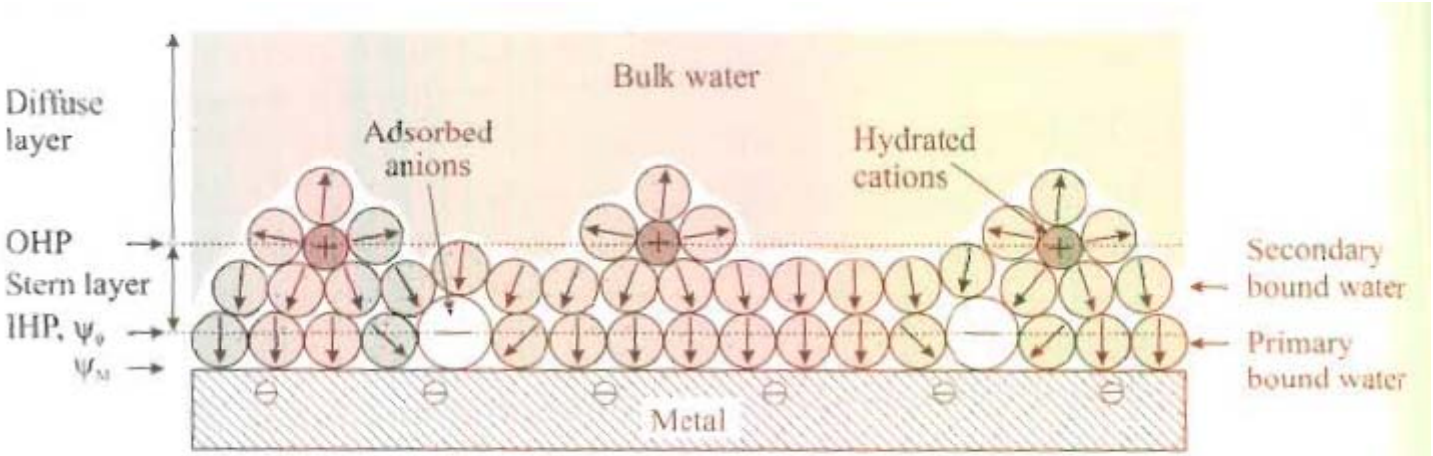

Figure 4.6: Stern layer at a metal surface. Due to the high electrical conductivity, the potential in the metal ψ_M is constant up to the surface. The inner (IHP) and outer (OHP) Helmholtz planes are indicated. In the first layer of primary bound water the permittivity is typically $\varepsilon = 6$. In the secondary layer of water it is of the order of $\varepsilon \approx 30$.

H. Butt, K. Graf, M Kapple, physics and chemistry of interface, WILEY-VCH (2006)

SOGANG UNIVERSITY

Charge inversion e.g. – PRL **97**, 046102 (2006)

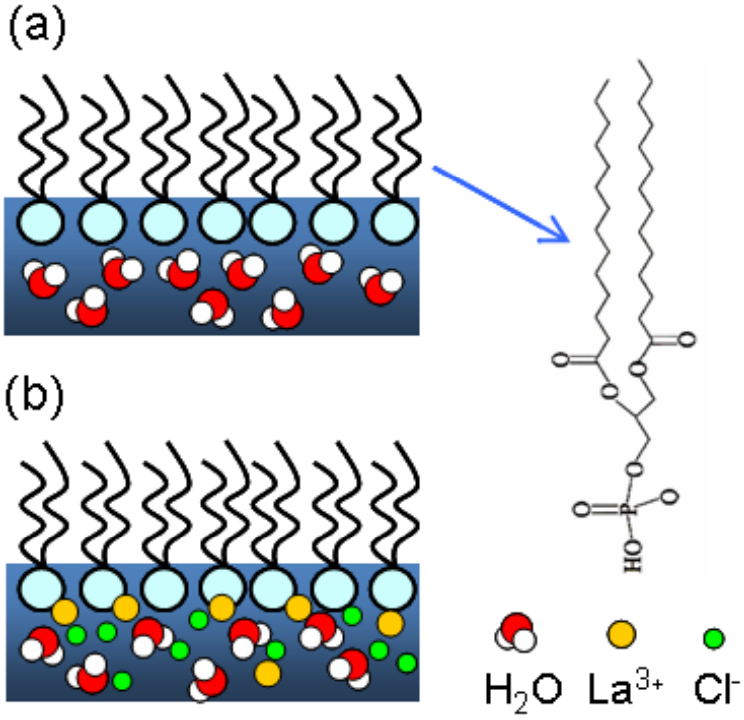

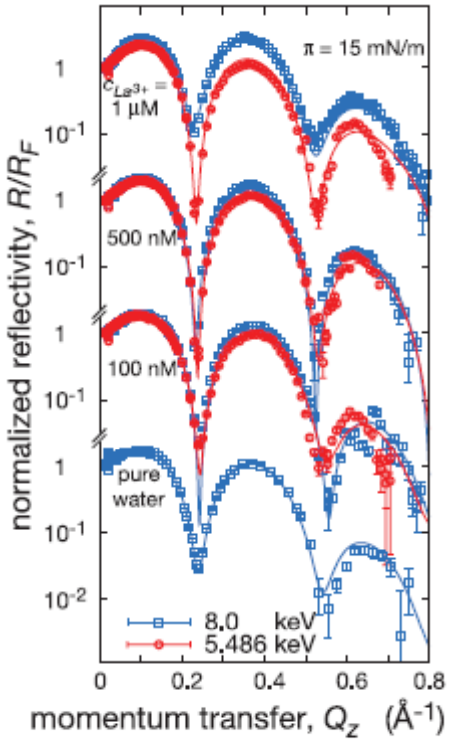

FIG. 2 (color). Fresnel-normalized x-ray reflectivities, R/R_F, of DMPA monolayers at $E = 8.0$ keV (off resonance) and 5.486 keV (La L_{III} resonance) on aqueous $LaCl_3$ solutions. For clarity, subsequent pairs of data sets are offset by a factor of 100 each. Solid lines derive from model fits.

SOGANG UNIVERSITY

Charge inversion e.g. – PRL **97**, 046102 (2006)

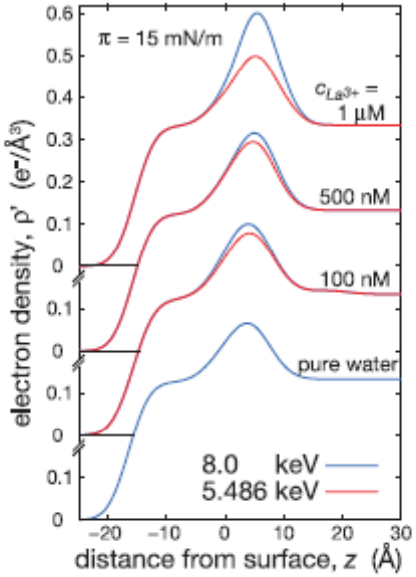

FIG. 3 (color). VRDF electron density profiles derived from fits to the experimental data. The off-resonance and on-resonance data shown in Fig. 2 were corefined with consistent sets of parameters that deviated only in the effective electron numbers and absorption cross sections of the La^{3+} component. Subsequent ED pairs are offset by $0.2e^{-}/Å^{3}$ for clarity. Similar ED profiles were derived from a modified box model as described in the text. The number density of La^{3+} at the interface was subsequently obtained from such models via Eq. (2).

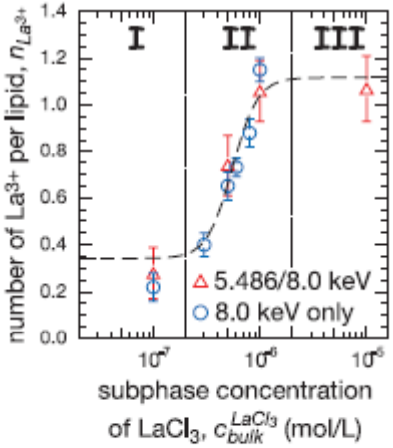

FIG. 4 (color). Number of adsorbed La^{3+} per DMPA in surface monolayers as a function of bulk $LaCl_3$ concentration. Red plot symbols indicate results at 15 mN/m derived from the anomalous reflectivity data pairs shown in Fig. 2 and ED profiles similar to those shown in Fig. 3. The results indicated by blue symbols were derived from independent data measured at 8.0 keV alone.

SOGANG UNIVERSITY